RELATIVE INFLUENCE OF MECHANICAL AND METEOROLOGICAL FACTORS ON AVALANCHE RELEASE DEPTH DISTRIBUTIONS: AN APPLICATION TO FRENCH ALPS

Johan Gaume, Guillaume Chambon*, Nicolas Eckert, Mohamed Naaim
IRSTEA, UR ETGR, Grenoble, France

ABSTRACT: The evaluation of avalanche release depth distributions represents a challenging issue for the mapping, zoning and long-term hazard management in mountainous regions. To that aim, both the distribution of snowfalls and the occurrence probability of an avalanche release for a given snow height need to be assessed. In this study, a rigorous formalism allowing coupling of these two ingredients into a mechanical-statistical model is presented. The stability criterion of a layered snowpack is investigated using a finite-element analysis accounting for the spatial heterogeneity of weak-layer mechanical properties, while the available snow depth is evaluated by studying the distribution of 3-day extreme snowfalls. The release depth distributions predicted by this coupled model are then compared to a well-documented database encompassing 369 natural slab avalanches recorded in La Plagne, France. It appears that with only one adjustable parameter, an excellent agreement can be obtained both for the power-law tail of the distribution, corresponding to large slab depths, and for its core corresponding to shallow slab depths. Two important conclusions can be drawn: (1) Small to medium-sized avalanches are controlled mainly by mechanics, whereas large avalanches are influenced by a strong mechanical-meteorological coupling. (2) The release depth distributions, including the value of the power-law exponent obtained for large slab depths, are highly variable in space and cannot be regarded as universal. Finally, the model is extended using a robust interpolation procedure in order to produce maps of expected release depths for different return periods.

1. INTRODUCTION

During the past decade, several studies have focused on the statistical distributions of slab avalanche release depths and surfaces (e.g., Rosenthal & Elder, 2002; McClung, 2003; Failletaz et al., 2006). In particular, the tail of these distributions, for large avalanches, has repeatedly been reported to follow a power-law trend. This led some authors to postulate the existence of a universal behaviour, although this universality is still a matter of debate (Bair et al., 2008). To shed new light on this issue, and eventually to be capable of evaluating avalanche release size distributions even in absence of data, a detailed investigation of the physical and mechanical processes giving rise to these distributions is required. It is commonly accepted that dry-snow slab avalanches are initiated by a shear failure in a weak-snow layer (or at a weak interface), followed by tensile crown failure of the overlying slab (McClung, 1979; Schweizer et al., 2003). The mechanical properties of the weak layer, in particular the strong spatial variability of these properties and the repartition of "weak spots" where failure initiate (Schweizer et al., 2008), can thus be expected to play a major role on avalanche size distributions. Another important ingredient to explain these distributions is meteorology, since the available snowfall represents an obvious limiting factor for avalanche depths.

The purpose of this proceeding is to report on the capabilities of a coupled mechanical–meteorological model for the prediction and understanding of slab avalanche size distributions. The meteorological factor is accounted for through a statistical distribution of extreme snowfalls. Regarding the mechanical model, since snow is a complex material whose mechanical behavior is still far from being fully understood, we chose to use constitutive laws as simple as possible while still incorporating all the physical ingredients necessary to produce realistic avalanche releases. In particular, on the base of previous studies (Schweizer, 1999; Failletaz et al., 2004; Fyffe & Zaiser, 2004, 2007), the following two key ingredients are taken into account: (1) the spatial variability of the weak layer mechanical properties, and (2) the long-range stress redistribution effects at the slab – weak layer interface mediated by the elasticity of the slab. Additional information concerning the coupled model developed can be found in Gaume et al. (2012a, 2012b).

* *Corresponding author address*: G. Chambon, IRSTEA (formerly Cemagref), Domaine Universitaire, BP 76, 38402 St-Martin-d'Hères Cedex, France; tel: (33)-47676-2766; email: guillaume.chambon@irstea.fr.

2. FINITE ELEMENT MECHANICAL MODEL

2.1 Model formulation

A mechanical model of slab avalanche release was developed using the open-source finite element code Cast3m. The simulated system consists of a 2D (plane stress conditions) slab of thickness h overlying a weak layer modeled as an interface of zero thickness (Fig. 1). The length of the slope is L = 50m, and it is inclined at an angle θ with the horizontal. The numerical mesh is composed of 100 elements in the slope-parallel direction x, and 6 elements in the cross-slope direction z. The system is loaded by progressively increasing the slope angle θ at constant slab height h until rupture.

The slab, constituted of cohesive snow, is modeled as an isotropic brittle-elastic material characterized by a Young's modulus E, a Poisson's ratio ν, and a tensile rupture strength σ_t. The weak layer is represented as an elasto-plastic strain-softening material. The interface relationship between the shear stress τ and the tangential displacement u has been taken linear piecewise. The shear stress peak τ_p is reached for a characteristic displacement u_p and is given by a Mohr-Coulomb criterion: $\tau_p = c + n \tan\phi$, where c is the cohesion, ϕ is the friction angle, and n is the normal stress. In the pre-peak phase, the interface is elastic with a tangential stiffness $k_s = \tau_p/u_p$. In the post-peak phase, the shear stress decreases (shear softening) until reaching a residual value $\tau_r = \sigma_n \tan\phi$ for a characteristic displacement $u_r = 2\ u_p$. This residual stress corresponds to the situation where ice bridges are completely broken and only the friction between the slab and the underlying layer remains.

The spatial heterogeneity of weak layer mechanical properties is accounted for through a stochastic distribution of cohesion c (Fig. 1). Following Jamieson & Johnston (2001) and Kronholm & Birkeland (2005), a Gaussian distribution of average $< c >$ and standard deviation σ_c is considered, while spatial correlations are represented by a spherical covariance function with a correlation length ε. Cohesion fields corresponding to different values of ε, in the range 0.5 – 40m, have been generated.

The values used for the various parameters involved in the model, which have been selected according to available data (Föhn et al., 1998; Schweizer, 1999; Schweizer et al., 2008), are summarized in Table 1. The model has been thoroughly validated against particular situations (weak layer heterogeneity reduced to localized weak spots of zero cohesion) for which analytical solutions can be obtained.

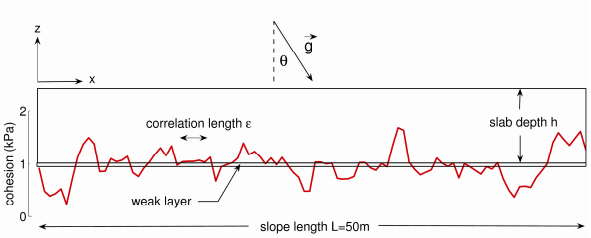

Figure 1: Geometry of the simulated system: a weak layer interface under a cohesive slab of depth h. A realization of the weak layer cohesion heterogeneity is also shown (case ε = 2m).

Table 1: Mechanical parameters used in the simulations for the slab and the weak layer (w.l.).

Parameter	Value
slab density ρ	250 kg.m^{-3}
slab Young modulus E	1 MPa
slab Poisson ratio ν	0.2
slab viscosity η	10^8 Pa.s
slab tensile strength σ_t	> 1500 Pa
w.l. average cohesion $\langle c \rangle$	1 kPa
w.l. cohesion std. deviation σ_c	30% $\times \langle c \rangle$
w.l. friction angle Φ	30°
w.l. displacement to failure u_p	2 mm
w.l. residual displacement u_r	4 mm
correlation length ϵ for w.l. cohesion variations	$0.5 - 40$ m

2.2 Avalanche release types

Two types of avalanche releases were distinguished in the simulations: full slope release, where the entire simulated slope is released without traction rupture within the slab; and partial slope release, where traction rupture occurs within the slab and hence only a part of the slope is released. As shown in Fig. 2, the relative proportion of these two types of releases for a given set of simulations is strongly dependent on the mechanical parameters used, and in particular on the slab tensile strength σ_t. Importantly, however, for both release types, the primary rupture process observed is always the shear failure of the weak layer. Slab traction rupture, when existent, systematically constitutes a secondary process. Hence, the statistical distributions of release angles are essentially unaffected by the release type. For the sake of simplicity, we thus focus in what follows on a single release type, namely full slope release. The

results presented henceforth have been obtained with values of σ_t sufficiently high to completely prevent traction rupture in the slab.

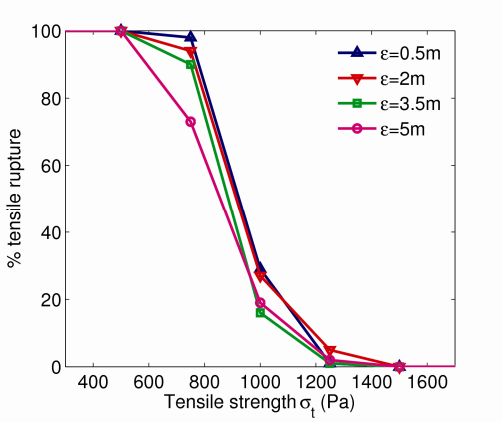

Figure 2: Relative proportion of partial slope releases within a given ensemble of simulations as a function of slab tensile strength σ_t and for different values of the weak layer cohesion correlation length ε (case h = 1m).

2.3 Release angle distributions

Fig. 3 shows the distributions of release angle θ_r obtained in the simulations, presented in terms of release factor $F = \sin\theta_r - \tan\phi\cos\theta_r$. First, it clearly appears that all release factor distributions can be well adjusted by Gaussian laws. We also observe that the average $< F >$ and the standard deviation σ_F of these distributions tend to decrease with the slab depth h. On the contrary, the average appears approximately independent of the correlation length ε, while the standard deviation increases with ε.

In detail, the average release factor is found to be accurately predicted by the following expression:

$$< F >= \frac{< c >}{\rho g h}, \qquad (1)$$

which corresponds to the result that would be obtained with homogeneous weak layer properties. Hence, the release factor averages are essentially unaffected by the weak layer heterogeneity.

Concerning the release factor standard deviation σ_F, it can be compared to the standard deviation $\sigma_\infty = \sigma_c / (\rho g h)$ that would be obtained in the case of a completely rigid slab (i.e. in the case where the stress field variations would exactly follow the weak layer heterogeneity). As shown in Fig. 4, the first important observation is that σ_F is always significantly lower than σ_∞. This highlights an effect of smoothing of the heterogeneity by the elasticity of the slab and the associated stress redistribution.

From theoretical analysis, it can be shown that the typical length scale over which this elastic smoothing effect is active, is given by (Gaume et al, 2012b):

$$\Lambda = \sqrt{\frac{E h u_p}{(1-\nu^2)\tau_p}}. \qquad (2)$$

As a consequence, it is found that σ_F can be expressed as:

$$\sigma_F = \sigma_\infty f(\varepsilon / \Lambda), \qquad (3)$$

where the function $f(\varepsilon / \Lambda)$ is well approximated by a power law in the range of parameters investigated (Fig. 4). The characteristic length Λ assumes typical values on the order of 1m in our simulations.

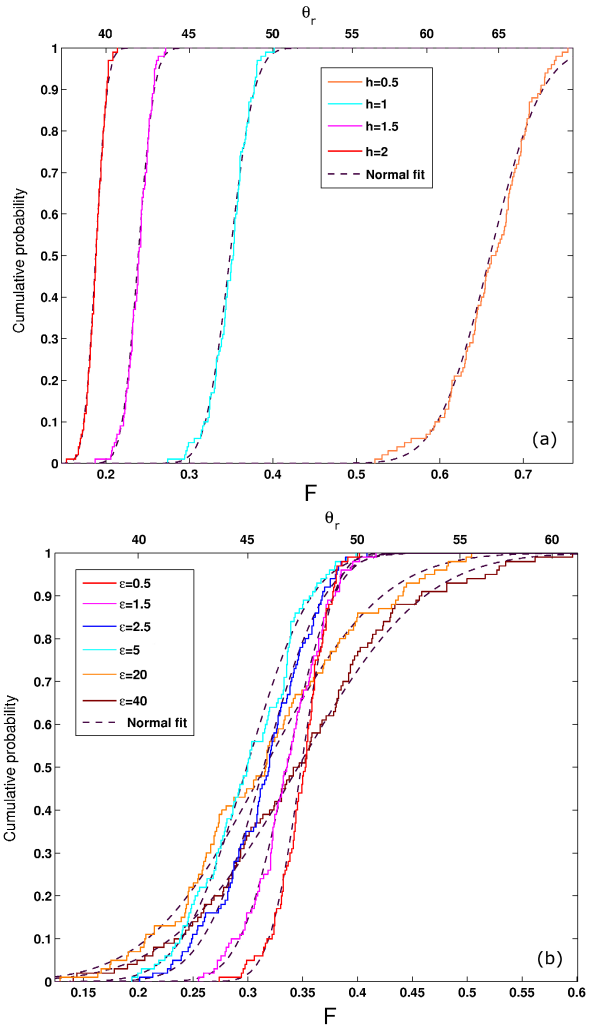

Figure 3: Cumulative distributions of release factor F. The top scale (non-linear) indicates the corresponding values of release angle θ_r. (a) ε = 0.5m and various values of slab depth h; (b) h = 1m and various values of correlation length ε.

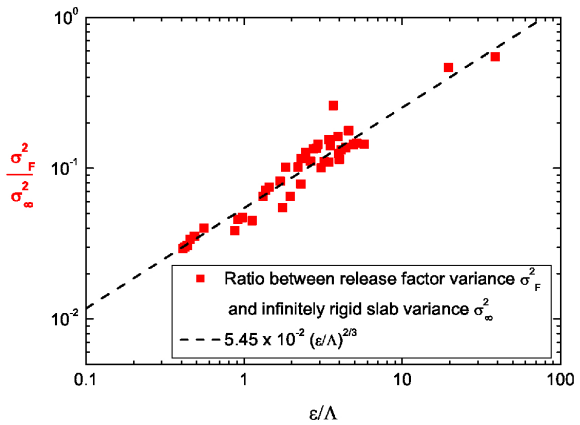

Figure 4: Ratio between release factor variance σ_F and infinitely rigid slab variance σ_∞ as a function of the ratio between the correlation length ε and the characteristic length Λ for all (h,ε) couples (approx. 5000 simulations).

2.4 Release depth distributions

From the distributions of release factor at fixed depth directly deduced from the simulations, the distributions of release depth that would be obtained at fixed slope angle can easily be derived. Indeed, the couples (h,θ_r) at avalanche release are independent of the loading procedure used. In particular, it can be shown that the release depth distributions do also approximately follow Gaussian laws with averages $< h >$ and standard deviations σ_h given by:

$$< h >= \frac{< c >}{\rho g F}, \tag{4}$$

$$\sigma_h = \frac{\sigma_c}{\rho g F} f(\varepsilon / \Lambda). \tag{5}$$

Once again, it is noteworthy that, due to the elastic smoothing effect, the standard deviation σ_h is much smaller than the one that would be obtained with a completely rigid slab, and increases with the correlation length ε.

Lastly, to be eventually compared with data which generally encompass avalanche paths of various slopes, these depth distributions at fixed angle need to be integrated over all possible slope values. In order to obtain an analytical expression for the integrated mechanical release depth distribution $p_m(h)$, and without significant loss of generality, this step was performed by assuming a uniform slope distribution between θ_{min} = 30° and θ_{max} = 90° (see Gaume et al., 2012a).

3. COUPLED MECHANICAL-METEOROLOGICAL MODEL

3.1 Coupling relationship

To obtain realistic avalanche release depth distributions, the release depth distribution $p_m(h)$ derived from the mechanical model has to be coupled to a statistical description of snowfalls. To that purpose, we postulate that a slab avalanche release can occur only if the available snow depth above the weak layer exceeds the release depth predicted by the mechanical model. It can then be shown that coupled release depth probability *p(h)* can be expressed as a function of the mechanical distribution $p_m(h)$ and the snowfall distribution $p_{sf}(h_{sf})$ as follows:

$$p(h) = \frac{p_m(h) p_{sf}(\geq h)}{C}, \tag{6}$$

where $p_{sf}(\geq h_{sf}) = \int_{h_{sf}}^{\infty} p_{sf}(h) dh$ is the snowfall cumulative exceedence distribution, and C is a normalization factor: $C = \int_0^{\infty} p_m(h) p_{sf}(\geq h) dh$. This coupling formulation makes evident that the global avalanche release depth probability $p(h)$ actually corresponds to the mechanical probability $p_m(h)$ weighted by the probability of having a snowfall h_{sf} greater than h.

3.2 Extreme snowfall distribution

It has been suggested in several studies (e.g., Schweizer et al., 2003; Bocchiola et al., 2006) that, for Northern Alps, the best indicator to forecast avalanche release is the three-day snowfall. Since, in addition, only extreme precipitations give rise to avalanches, we chose to identify $p_{sf}(h_{sf})$ with the distribution of three-day snowfall annual maxima, which can be described by a Generalized Extreme Value (GEV) function:

$$p_{sf}(\geq h_{sf}) = 1 - \exp\left[-\left(1 + \xi \frac{h_{sf} - \mu}{\sigma} \right)^{-1/\xi} \right], \tag{7}$$

where μ, σ, and ξ are, respectively, the location, scale, and shape parameters. These three parameters depend on the site considered.

3.3 Comparison with La Plagne (France) data

Ski patrollers from La Plagne (France) ski resort provided us with a database collecting geometrical and physical characteristics of 14,391 avalanches that occurred from winters 1998 to 2010. From the

complete database, 369 natural slab avalanches were extracted. In agreement with previous studies (Rosenthal & Elder, 2002; McClung, 2003; Failletaz et al., 2006), we found that the tail of the release depth cumulative exceedence distribution (c.e.d.) of these avalanches appears to follow a power-law.

Fig. 5 shows the comparison between these field data and the release depth distribution predicted by the coupled mechanical-meteorological model. For this application, values of the GEV parameters relevant to the considered site have been used: μ = 0.98m, σ = 0.21m, and ξ = 0.214. Only the mechanical cutoff $h_m = [< c > - 2\sigma_c f(\varepsilon / \Lambda_0)]/(\rho g)$ (see Fig. 5), which depends on a combination of the different mechanical parameters, has been adjusted to improve the match with the data. The final value retained, namely h_m = 0.18m, corresponds to values of $< c > = 0.6$kPa, $\sigma_c/< c > =$ 30%, and ε = 2m which are fully consistent with existing measurements on snow. We observe that with this single adjustable parameter, the presented model is capable of reproducing La Plagne data with a remarkable accuracy. Not only the power-law tail of the c.e.d., corresponding to large slab depths, but also the core of the distribution for lower slab depths, are well captured.

It can be noted that the individual mechanical and meteorological distributions both present significant discrepancies with the data (Fig. 5). Hence, the coupling between these two ingredients appears as really essential to understanding natural slab avalanche releases. In detail, three different zones can be distinguished on the coupled probability $p(h)$. Below the mechanical cutoff, for $h < h_m$, no avalanche can occur. For small to medium-sized avalanches ($h_m \leq h \leq h_s$, where h_s denotes the cutoff appearing on the snowfall distribution), the coupled c.e.d. shows a concave shape (in log-log scales). This zone corresponds to a regime of weak coupling where the release depth probability is essentially controlled by the mechanical probability. Lastly, large avalanches ($h > h_s$) correspond to a regime of strong coupling where the snowfall thickness plays the role of a limiting factor on the mechanical probability. In this regime, the model effectively predicts a power-law shape for the coupled c.e.d. $p(h)$.

From the model, the following expression can be derived for the exponent α of the c.e.d. power-law tail:

$$\alpha = -1 - 1/\xi, \qquad (8)$$

where the term −1 represents the mechanical contribution and the term $-1/\xi$ corresponds to the meteorological contribution. This exponent thus appears to be strongly dependent on the shape parameter ξ of the extreme snowfalls, which is itself highly variable in space. Hence, in agreement with the conclusions of Bair et al. (2008), the mechanical-meteorological model developed in this study clearly demonstrates that the shape of avalanche release depth distributions cannot be expected to be universal.

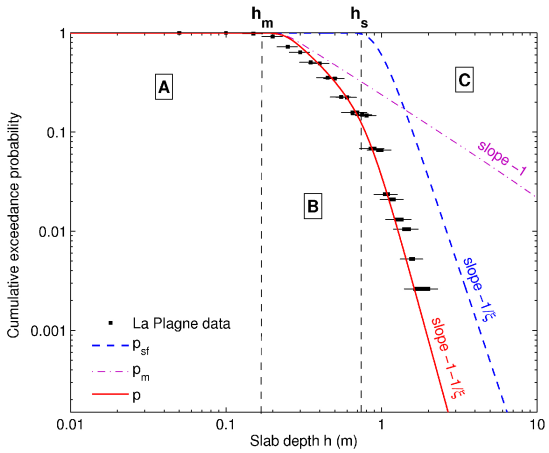

Figure 5: Mechanical release depth c.e.d. $p_m(h)$, extreme snowfall c.e.d. p_{sf} (h), and slab release depth c.e.d. predicted by the coupled model $p(h)$, compared with field release depth data from La Plagne.

4. CONCLUSIONS

The presented study evidences the relative roles played by the mechanical and meteorological factors on avalanche release depth distributions. Using a coupled mechanical-meteorological model, we were able to reproduce with excellent accuracy the release depth distributions of natural slab avalanches in La Plagne (France). For the first time, both the power-law tail as well as the whole core of the distribution are well captured, and this with only one adjustable parameter. This success can be viewed as a strong validation of the developed model, and confirms that the processes accounted for (mechanical heterogeneity, stress redistribution, and extreme snowfall distribution) effectively constitute the key ingredients to understand slab avalanche release. An important outcome is the strong spatial variability, and the non-universality, of the release depth distributions predicted.

The model developed can now be used to evaluate avalanche release depth distributions in

any given location, at the scale of the path or of an ensemble of paths (slope integration), provided the relevant meteorological and mechanical parameters are known. As an illustration, slope-integrated avalanche release depths corresponding to a return period of 100 years have been computed in the whole French Alps, using a robust max-stable procedure to interpolate the available extreme snowfall data (Eckert et al., 2011) and assuming a constant value for the mechanical cutoff h_m: see Fig. 6. Such type of predictions can then be directly input into avalanche propagation models, for instance, and might thus be extremely useful for avalanche hazard assessment and risk management in mountainous regions.

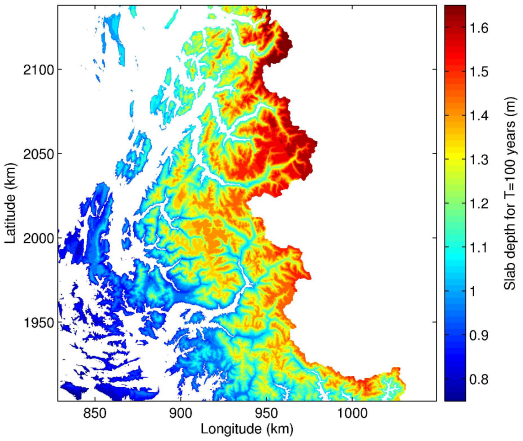

Figure 6: Slab avalanche release depths predicted by the model in the French Alps for a return period of 100 years.

ACKNOWLEDGMENTS

Support from the Interreg projects DYNAVAL and MAP^3 is acknowledged. We also express our gratitude to C. Schneider, snow expert in La Plagne, for providing release depth data.

REFERENCES

Bair, E. H., J. Dozier, and K. W. Birkeland (2008), Avalanche crown-depth distributions, *Geophys. Res. Lett.*, 35, L23502.

Bocchiola, D., M. Medagliani, and R. Rosso (2006), Regional snow depth frequency curves for avalanche hazard mapping in central Italian Alps, *Cold Reg. Sci. Technol.*, 46, 204221.

Eckert, N., J. Gaume, and H. Castebrunet (2011), Using spatial and spatial extremes to characterize snow avalanche cycles, *Procedia Environ. Sci.*, 7, 224–229.

Failletaz, J., F. Louchet, and J. Grasso (2004), Two-threshold model for scaling laws of noninteracting snow avalanches, *Phys. Rev. Lett.*, 93, 208001.

Failletaz, J., F. Louchet, and J. Grasso (2006), Cellular automaton modelling of slab avalanche triggering mechanisms: From the universal statistical behaviour to particular cases, in *Proceedings of the ISSW 2006*, pp. 174–180.

Föhn, P., C. Camponovo, and G. Krst (1998), Mechanical and structural properties of weak snow layers measured in situ, *Ann. Glaciol.*, 26, 1–6.

Fyffe, B., and M. Zaiser (2004), The effects of snow variability on slab avalanche release, *Cold Reg. Sci. Technol.*, 40, 229–242.

Fyffe, B., and M. Zaiser (2007), Interplay of basal shear fracture and slab rupture in slab avalanche release, *Cold Reg. Sci. Technol.*, 49, 26-38.

Gaume, J., G. Chambon, N. Eckert, and M. Naaim (2012a), Relative influence of mechanical and meteorological factors on avalanche release depth distributions: An application to French Alps, *Geophys. Res. Lett.*, 39, L12401.

Gaume, J., G. Chambon, N. Eckert, and M. Naaim (2012b), Influence of weak-layer heterogeneity on snow slab avalanche release: Application to the evaluation of avalanche release depth, manuscript in preparation.

Jamieson, J., and C. Johnston (2001), Evaluation of the shear frame test for weak snowpack layers, *Ann. Glaciol.*, 32, 59–69.

Kronholm, K., and K. Birkeland (2005), Integrating spatial patterns into a snow avalanche cellular automata model, *Geophys. Res. Lett.*, 32, L19504.

McClung, D. (1979), Shear fracture precipitated by strain softening as a mechanism of dry slab avalanche release, *J. Geophys. Res.*, 84, 3519–3526.

McClung, D. (2003), Size scaling for dry snow slab release, *J. Geophys. Res.*, 108, 2465.

Rosenthal, W., and K. Elder (2003), Evidence of chaos in slab avalanching, *Cold Reg. Sci. Technol.*, 37, 243–253.

Schweizer, J. (1999), Review of dry snow slab avalanche release, *Cold Reg. Sci. Technol.*, 30, 43–57.

Schweizer, J., J. Bruce Jamieson, and M. Schneebeli (2003), Snow avalanche formation, *Rev. Geophys.*, 41, 1016.

Schweizer, J., K. Kronholm, J. Jamieson, and K. Birkeland (2008), Review of spatial variability of snowpack properties and its importance for avalanche formation, *Cold Reg. Sci. Technol.*, 51, 253–272.